International Conference on Artificial Reality and Telexistence
Eurographics Symposium on Virtual Environments (2018)
G. Bruder, S. Cobb, and S. Yoshimoto (Editors)

Equivalent Physical Constant Hypothesis for Skill Transmission in Scale Conversion Telexistence

Hiroki Miyamoto[1], Masahiro Furukawa[1,2,3], Kosuke Wada[1], Masataka Kurokawa[1], Kohei Matsumoto[1], and Taro Maeda[1,2]

[1]Osaka University, Japan
[2]CiNet: Center for Information and Neural Networks, Japan
[3]JST, PRESTO, Japan

Abstract

Scale conversion telexistence can have an inconsistency in the motions of a human and robot of different scales. We assumed that the inconsistency is caused by the different apparent physical constants for the human and robot. We propose an equivalent physical constant hypothesis for motion skill transmission, which we verified experimentally by transmitting the standing-up movement of a human to a small robot. The robot successfully managed to stand up by compensating for the gravity. This proves the validity of the hypothesis.

CCS Concepts

• ***Embedded and cyber-physical systems*** → *Robotic control;*

1. Introduction

Many remotely operated robots have been realized not only for life rescue and extreme environmental work but also for communication with people. Replacing a person with a robot in a workspace and remotely steering the robot will enhance the pilot safety and shorten the travel time. Telexistence [Tac15] is a technology that makes maximum use of a human's judgment and motor skills. It refers to a robot working in the real world in real-time, but a human appears to be present instead of the robot. This is realized by visuo-motor coupling between the operator and surrogate robot.

Regarding the visual scale conversion of telexistence, changing the interocular or interpupillary distance of the binocular camera used for visual transmission has been reported to make a human feel like the size of the body changed [YT02] [BS11] [KI17]. These reports are based on the geometric similarity rule. However, because it is difficult to convert scales of physical constants and time with only the geometric similarity law, when interference or active motion of an object occurs, there is a mismatch between the movements of the person and robot owing to the difference in their sizes. A kinematic similarity law [TTK*07] has been considered that involves scaling physical constants and time. An example of a motion that requires the conversion of physical constants according to the environment is a lunar surface simulator [Spa70]. A kinematic similarity rule needs to be built for scale conversion telexistence.

We hypothesize that, if a physical constant applicable only on the robot side is made equivalent on the human side so that the robot's motion matches that of the person, telexistence should be realized even with scale conversion, and it will be possible to transmit conventional self-motor skills. We verified this hypothesis by considering the standing-up motion of a bipedal walking robot, which is significantly influenced by the apparent gravity.

2. Telexistence with a biped walking robot

A bipedal walking robot generally differs from a human in its degrees of freedom and mass distribution. Thus, measures need to be taken to maintain balance. For example, V-sido OS (Asratec Corp.) prevents falling by modifying the robot's motion in real time to another action that can help maintain balance.

For telexistence, movement is limited to the motions of the wheels or pattern walking by command inputs [TKS*03]. A method for a robot to move similarly to a human has not yet been reported. This may be because it is difficult to compensate for the parameters within ranges that do not deviate from those pertaining to the humanoid robot while maintaining behavior consistent with that of a human. For example, the bipedal walking robot WL-12 series has a leg length equivalent to that of a person and involves a body mechanism that accounts for 30% of the total weight of the robot; this mechanism corresponds to only the lower limbs and performs moment compensation by waving the body. In this case, the researchers successfully compensated for the bipedal pattern walking around three axes: roll, pitch [ToLTK90] [TTKK90], and yaw [YTK93].

Although not an example of a walking robot, Murataseisaku-kun (Murata Manufacturing Co.) is a small robot that compensates for the moment around the roll axis by using a high-speed rotating

DOI: 10.2312/egve.20181314

body, which helps in maintain balance. Thus, it does not have restrictions on the movable range for moment compensation. In this study, we assumed that the apparent physical constants of the robot match those of a person, so the influence due to the difference in dimensions can be neglected. This should make it objectively possible for the robot to exceed the capacity of humanoids and subjectively possible to maintain balance while maintaining human characteristics. For the posture tracking control of robots at scales different to that of humans, the robot's movements are matched to that of the person by adding a control to match apparent physical constants. We therefore hypothesize that telexistence can be realized while maintaining human existence even with robots of different scales.

3. Proposed approach

3.1. Equivalent physical constant hypothesis

The closer the movement of the body in the field of view matches the somatosensory characteristics, the stronger the existence that is experienced by the human. A stronger existence makes intuitive maneuvering possible. With scale conversion, however, all of the apparent physical constants are different, so inconsistencies in motion occur.

Three elements need to be considered for a telexistence via a robot with a scale different from that of a human: mechanical, visual, and physical. Mechanical elements involve matching the position-following ability and robot control [TTK*07], such as hand-eye coordination. Visual elements refer to the scale conversion of the self-body image because of changes in the interocular distance or interpupillary distance of the binocular camera [YT02] [BS11] [KI17]. Physical elements refer to the conversion of physical constants owing to scale differences [Spa70].

We propose the equivalent physical constant hypothesis for the scale conversion of physical elements in scale conversion telexistence, which is as follows. By adding a control that makes the apparent physical constants coincide with the robot attitude tracking control by a person of a different scale, the motions of the person and robot coincide. As a result, telexistence can be realized even with different-scale robots. To examine this hypothesis, we focused on gravity, which is the most dominant physical constant for balance control.

If a robot is modeled as an inverted pendulum of one link, it can be discussed in terms of the angular acceleration around the ground point. If the control law for the angular acceleration to match the vicinity of the ground contact point can be realized with a mechanism that does not hinder the immersive feeling of telexistence, the equivalent gravity condition for scale conversion telexistence is satisfied. In this study, we used a human 1/4-scale robot as a model. As a three-axis moment compensation device, we assumed a model in which three actuators are arranged so that their axes are orthogonal and a mass of m kg is placed at the tip of a link of l m extending vertically upward from the back of the robot.

3.2. Dynamic compensation model for the standing attitude

A moving human or robot can be considered as a rigid body, inverted pendulum with one link, arbitrary robot body, and balancer capable of compensating for any moment along the three axes. Figure 1 shows such a model and the equivalent human model. Table 1 defines the parameters. The center of gravity (CoG) $\boldsymbol{s}_i$, inertia tensor $\boldsymbol{I}_i$, and angular velocity $\boldsymbol{\omega}_i$ are determined by calculating the forward dynamics from a mounted gyro sensor and the robot's own posture.

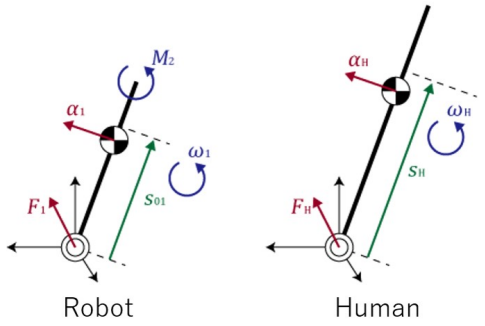

Figure 1: *Forces during the standing-up motion.*

Table 1: *Parameters of the dynamic compensation model.*

	Robot	Human	
Position Vector	$\boldsymbol{s}_{01}$,$\boldsymbol{s}_{12}$	$\boldsymbol{s}_H$	Known
Mass	m_1	m_H	
Inertia tensor around the CoG	$\boldsymbol{I}_1$	$\boldsymbol{I}_H$	
Angular velocity	$\boldsymbol{\omega}_1$	$\boldsymbol{\omega}_H$	
Translational acceleration of the CoG	$\boldsymbol{\alpha}_1$	$\boldsymbol{\alpha}_H$	Unknown
Translation force applied to the joint	$\boldsymbol{F}_1$	$\boldsymbol{F}_H$	
Angular acceleration of the CoG	$\dot{\boldsymbol{\omega}}_1$	$\dot{\boldsymbol{\omega}}_H$	
Joint torque	$\boldsymbol{\tau}_1$	$\boldsymbol{\tau}_H$	
Moment generated by the balancer	$\boldsymbol{M}_2$	-	

The procedure for matching the apparent gravity is as follows. First, the equation of motion of the human model is used to obtain the angular acceleration $\dot{\boldsymbol{\omega}}_H$ by which a person collapses under the condition of 1 G considering the forward dynamics. The torque $\boldsymbol{\tau}_H$ generated on the ankle is assumed to be sufficiently smaller than the gravity term, and $\boldsymbol{\tau}_H = 0$. Then, an equation of motion is established for the robot model that includes the occurrence moment $\boldsymbol{M}_2$ by the balancer. Similar to in the previous case, $\boldsymbol{\tau}_1 = 0$. The following constraint is also assigned to the angular acceleration $\dot{\boldsymbol{\omega}}_1$ under the condition that the robot body falls at an apparent gravity of 1 G:

$$\dot{\boldsymbol{\omega}}_1 = \dot{\boldsymbol{\omega}}_H \tag{1}$$

Then, the moment $\boldsymbol{M}_2$ to be generated by the balancer is obtained according to inverse dynamics. Generating this moment by the balancer establishes the equivalent gravity condition for the robot. In the standing model, the initial angle and initial angular velocity around the ground point of the CoG of the robot body and person are both set to 0.

3.3. Control law

3.3.1. Dynamic compensation model with a balancer

If a robot is represented as an inverted pendulum with one link, a robot model with a balancer can be regarded as an inverted pendulum with two links, as shown in Figure 2.

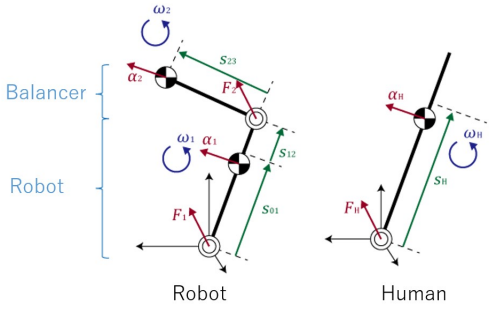

Figure 2: *(Left) Modeling of robot's dynamics including the balancer attached to its backside; (right) Modeling of human's dynamics*

The parameters used in this model are listed in Table 2. $|\boldsymbol{s}_{23}|$ is a constant corresponding to the shape of the balancer. In order to compensate for the moment, the output torque $\boldsymbol{\tau}_2$ of the balancer is controlled. The control equation is obtained with the method defined in the previous section.

Table 2: *Parameters of the dynamic compensation model with the balancer.*

	Robot	Balancer	Human	
Position Vector	$\boldsymbol{s}_{01}$,$\boldsymbol{s}_{12}$	$\boldsymbol{s}_{23}$	$\boldsymbol{s}_H$	
Mass	m_1	m_2	m_H	
Inertia tensor around the CoG	$\boldsymbol{I}_1$	$\boldsymbol{I}_2$	$\boldsymbol{I}_H$	Known
Angular velocity	$\boldsymbol{\omega}_1$	$\boldsymbol{\omega}_2$	$\boldsymbol{\omega}_H$	
Translational acceleration of the CoG	$\boldsymbol{\alpha}_1$	$\boldsymbol{\alpha}_1$	$\boldsymbol{\alpha}_H$	
Translation force applied to the joint	$\boldsymbol{F}_1$	$\boldsymbol{F}_2$	$\boldsymbol{F}_H$	Unknown
Angular acceleration of the CoG	$\dot{\boldsymbol{\omega}}_1$	$\dot{\boldsymbol{\omega}}_2$	$\dot{\boldsymbol{\omega}}_H$	
Joint torque	$\boldsymbol{\tau}_1$	$\boldsymbol{\tau}_2$	$\boldsymbol{\tau}_H$	

3.3.2. Forward dynamics of the human model

In order to generate the angular acceleration $\dot{\boldsymbol{\omega}}_H$ on the human, an equation of motion is established for one link based on the equations of rotational and translational equilibrium for the human model:

$$\boldsymbol{\tau}_H + (-\boldsymbol{s}_H) \times \boldsymbol{F}_H = \frac{\mathrm{d}}{\mathrm{d}t}(\boldsymbol{I}_H \boldsymbol{\omega}_H) \tag{2}$$

$$\boldsymbol{F}_H + m_H \boldsymbol{g} = m_H \boldsymbol{\alpha}_H \tag{3}$$

Because the input torque by the ankle is sufficiently smaller than the gravity term, $\boldsymbol{\tau}_H = 0$.

$$\boldsymbol{I}_H \dot{\boldsymbol{\omega}}_H = -m_H \boldsymbol{s}_H \times (\dot{\boldsymbol{\omega}}_H \times \boldsymbol{s}_H) + m_H \boldsymbol{s}_H \times \boldsymbol{g} - \boldsymbol{\omega}_H \times (\boldsymbol{I}_H \boldsymbol{\omega}_H) \tag{4}$$

By comparing each component with the terms in Equation (4), the angular acceleration $\dot{\boldsymbol{\omega}}_H$ generated under an apparent gravity of 1 G is obtained. In addition,

$$\dot{\boldsymbol{\omega}} = \begin{bmatrix} \dot{\omega}_x \\ \dot{\omega}_y \\ \dot{\omega}_z \end{bmatrix}, \boldsymbol{s} = \begin{bmatrix} x \\ y \\ z \end{bmatrix} \tag{5}$$

Then,

$$\boldsymbol{s} \times (\dot{\boldsymbol{\omega}} \times \boldsymbol{s}) = (\boldsymbol{s} \cdot \boldsymbol{s})\dot{\boldsymbol{\omega}} - (\boldsymbol{s} \cdot \dot{\boldsymbol{\omega}})\boldsymbol{s} = \boldsymbol{T}_s \dot{\boldsymbol{\omega}} \quad (\boldsymbol{T}_s \text{ is known matrix}) \tag{6}$$

For the sake of simplicity, the subscripts are removed. The known vectors can then be used to define $\boldsymbol{k}$ as follows:

$$(\boldsymbol{I} + m\boldsymbol{T}_s)\dot{\boldsymbol{\omega}} = \boldsymbol{k} \tag{7}$$

Multiplying both sides by $(\boldsymbol{I} + m\boldsymbol{T}_s)^{-1}$ obtains $\dot{\boldsymbol{\omega}}_H$.

3.3.3. Inverse dynamics of the robot model

The following constraint condition is set so that the angular acceleration of the robot's main body matches that of the person:

$$\dot{\boldsymbol{\omega}}_1 = \dot{\boldsymbol{\omega}}_H \tag{8}$$

In order to obtain the torque $\boldsymbol{\tau}_2$ generated by the balancer to satisfy this condition, an equation of motion for two links is established based on the equations of rotation and translation for the robot model:

$$\boldsymbol{\tau}_1 + (-\boldsymbol{s}_{01}) \times \boldsymbol{F}_1 - \boldsymbol{\tau}_2 + \boldsymbol{s}_{12} \times (-\boldsymbol{F}_2) = \frac{\mathrm{d}}{\mathrm{d}t}(\boldsymbol{I}_1 \boldsymbol{\omega}_1) \tag{9}$$

$$\boldsymbol{\tau}_2 + (-\boldsymbol{s}_{23}) \times \boldsymbol{F}_2 = \frac{\mathrm{d}}{\mathrm{d}t}(\boldsymbol{I}_2 \boldsymbol{\omega}_2) \tag{10}$$

$$\boldsymbol{F}_1 + (-\boldsymbol{F}_2) + m_1 \boldsymbol{g} = m_1 \boldsymbol{\alpha}_1 \tag{11}$$

$$\boldsymbol{F}_2 + m_2 \boldsymbol{g} = m_2 \boldsymbol{\alpha}_2 \tag{12}$$

When the ankle torque $\boldsymbol{\tau}_1 = 0$ and known vectors $\boldsymbol{k}_1$ and $\boldsymbol{k}_2$ are used, the following can be obtained:

$$-m_2 \boldsymbol{s}_{02} \times (\dot{\boldsymbol{\omega}}_2 \times \boldsymbol{s}_{23}) - \boldsymbol{\tau}_2 = \boldsymbol{k}_1 \tag{13}$$

$$-m_2 \boldsymbol{s}_{23} \times (\dot{\boldsymbol{\omega}}_2 \times \boldsymbol{s}_{23}) + \boldsymbol{\tau}_2 = \boldsymbol{I}_2 \dot{\boldsymbol{\omega}}_2 + \boldsymbol{k}_2 \tag{14}$$

We define

$$\dot{\boldsymbol{\omega}} = \begin{bmatrix} \dot{\omega}_x \\ \dot{\omega}_y \\ \dot{\omega}_z \end{bmatrix}, \boldsymbol{s}_{02} = \begin{bmatrix} x_a \\ y_a \\ z_a \end{bmatrix}, \boldsymbol{s}_{23} = \begin{bmatrix} x_b \\ y_b \\ z_b \end{bmatrix} \tag{15}$$

Then,

$$\boldsymbol{s}_{02} \times (\dot{\boldsymbol{\omega}} \times \boldsymbol{s}_{23}) = \boldsymbol{T}_a \dot{\boldsymbol{\omega}} \quad (\boldsymbol{T}_a \text{ is known matrix}) \tag{16}$$

$$\boldsymbol{s}_{23} \times (\dot{\boldsymbol{\omega}} \times \boldsymbol{s}_{23}) = \boldsymbol{T}_b \dot{\boldsymbol{\omega}} \quad (\boldsymbol{T}_b \text{ is known matrix}) \tag{17}$$

In addition, we define the known matrices $\boldsymbol{A}$ and $\boldsymbol{B}$ as

$$\boldsymbol{A} = -m_2 \boldsymbol{T}_a, \quad \boldsymbol{B} = (\boldsymbol{I}_2 + m_2 \boldsymbol{T}_b) \tag{18}$$

Then, Equations (9) and (10) can be expressed as follows:

$$\boldsymbol{\tau}_2 = \boldsymbol{A}\dot{\boldsymbol{\omega}}_2 - \boldsymbol{k}_1 \tag{19}$$

$$\boldsymbol{\tau}_2 = \boldsymbol{B}\dot{\boldsymbol{\omega}}_2 + \boldsymbol{k}_2 \tag{20}$$

The determinant of $\boldsymbol{T}_a$ is always 0. Because $\boldsymbol{A}$ does not have an inverse matrix, the torque $\boldsymbol{\tau}_2$ is obtained as follows:

$$\boldsymbol{\tau}_2 = (\boldsymbol{A}\boldsymbol{B}^{-1} - \boldsymbol{E})^{-1}(\boldsymbol{k}_1 + \boldsymbol{A}\boldsymbol{B}^{-1}\boldsymbol{k}_2) \quad (21)$$

4. Scale conversion telexistence system

4.1. Function of the balancer during the standing-up motion

Figure 3 shows the standing-up motion models of a robot with a balancer and of a human. If the balancer does not function as the 1/4-scale robot stands up, the backward moment due to gravity is too large, and the waist ground point floats rather than the contact point of the foot sole. Therefore, the balancer moves to generate a forward moment in accordance with the control law defined in the previous section.

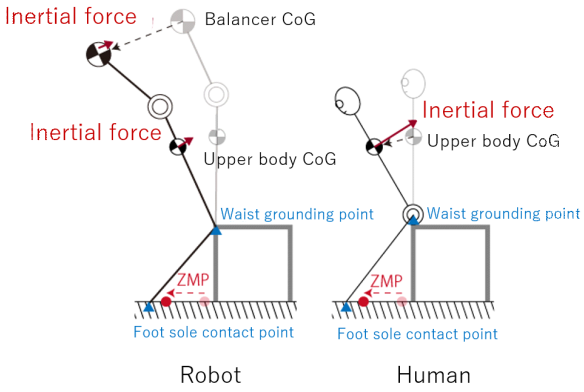

Figure 3: *Operation of the balancer during the standing-up motion.*

4.2. Demonstration machine

4.2.1. Small slave robot

In this study, we used a robot based on KHR-3HV (Kondo Kagaku) as a 1/4-scale slave robot. This robot can be regarded as two links: the main body and balancer. Additionally, the angle and angular velocity information about the three axes were acquired with the gyroscopic sensor MPU-6050 (InvenSense) for each link. The body part, including the support part of the balancer, has a height of 0.400 m and mass of 1.72 kg. Figure 4 shows the robot.

The robot has 29 degrees of freedom (DOF): three for the neck, five for each arm, one for the waist, six for each leg, and three for the balancer. Figure 5 shows the DOF configuration of the robot.

Binocular cameras were mounted on the head of the robot, and the interocular distance was set to 16.0 mm, which is 1/4 the eye distance of an average person (i.e., 65.0 mm).

To transmit the standing up skill, a flat wooden board with a rubber ground surface and dimensions of a 70.0 mm length, 60.0 mm width, and 8 mm thickness was used on the bottom of the robot's foot. Multiplying this length by four becomes 280 mm, so a person

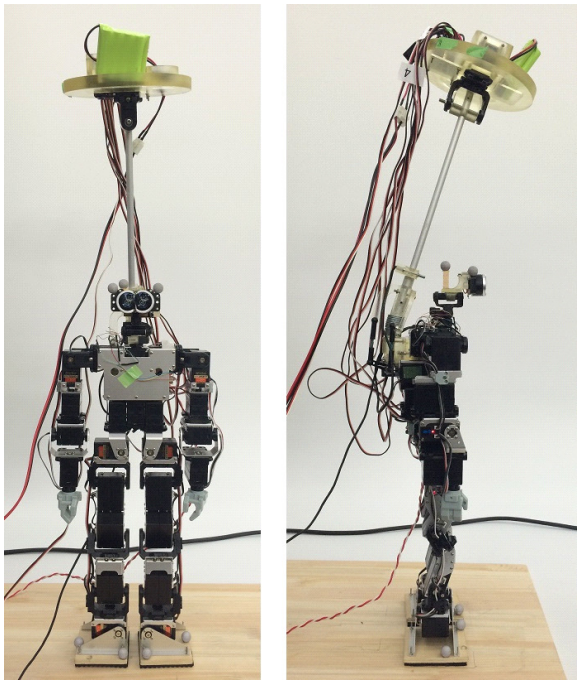

Figure 4: *Small slave robot.*

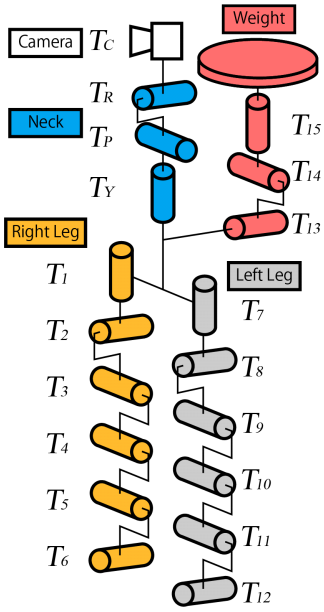

Figure 5: *DOF configuration.*

can behave as if wearing shoes that are 28.0 cm in size. Figure 6 shows the robot's foot.

As a control strategy, foot-eye coordination was used so that the relative positions of the head and foot were in-line with each other. The highest priority was to match the movements of the toe in the field of view for the human and robot. In addition, the body was

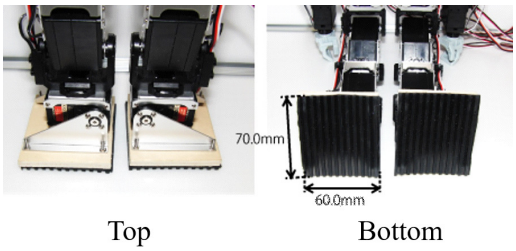

Figure 6: *Robot's foot.*

fixed in a direction perpendicular to the ground to simplify compensation control and prioritize real-time control. As long as the legs were stably grounded, the optical flow of the scaled robot was equivalent to the case of a human seeing the world with the naked eye. A strong existence was expected to be obtained.

4.2.2. Three-axis moment compensation mechanism

The three-axis moment compensation machine had a mass of 0.475 kg at the tip of the 0.350 m link. The movable range of the roll and pitch axes was $\pm 33.0^{\circ}$ from the base. The rotating shaft used the KRS-2572HV ICS (Kondo Kagaku) as a geared motor, and the current was controlled with a DA conversion board PCI-6229 (National Instrument) and motor driver JW-143-2 (Okatech). The moment of inertia of this machine with respect to the roll and pitch axes was obtained with the two-point hanging method. This was used to obtain the frequency $f = 0.808$ Hz and moment of inertia around the CoG $J = 0.00402$ kgm^2. The equilibrium axis theorem was used to calculate the moment around the axis of rotation of the balancer $J_0 = 0.0462$ kgm^2.

4.2.3. Master device

The optical motion capture system Opti Track (Natural Point) was used as the master system. We placed markers on the head (HMD), right hand, and feet. The visual field information of the robot was output to an Oculus Rift (OculusVR) worn by the person in real-time. In order to reduce the model error due to deformation of the human's shoes, a wooden board with a length of 280 mm and width of 260 mm (four times as large as the sole of the robot) was attached to the sole of the human.

4.3. Transmission of the standing-up motion

In order to verify the effect of equivalent physical conditions, the standing-up motion of the person measured under a gravitational acceleration of 1 G was transmitted to the 1/4-scale robot with and without apparent gravity compensation. This motion was evaluated according to the trajectory of the viewpoint height.

4.3.1. Experiment 1: Transmission of the standing-up motion under an apparent gravity of 4 G

A standing-up experiment with 1/4-scale conversion telexistence under an apparent gravity of 4 G was performed to represent no gravity compensation.

A human performed exercises while obtaining visual feedback from the robot. For the human motion, four markers were measured at 30 Hz. The distance between the markers was scaled by 1/4, and the rotation angle was retained. The robot followed the human's attitude.

The link length and mass of the person were 1.73 m and 60 kg, respectively, and those of the robot body were 0.40 m and 1.91 kg. The height of the chair was 0.75 m for the human and 0.19 m for the robot. The sense of telexistence was monitored by following the head during the sitting-down motion.

The subject was instructed to stand up as soon as possible while balancing with the upper body to not fall over. The standing-up motion by the robot was judged to be successful when the back of the shielded object could be visualized (Figure 7).

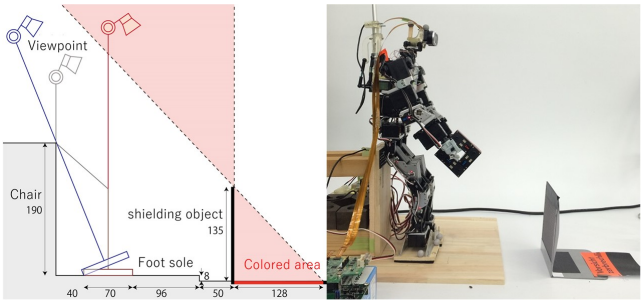

Figure 7: *(Left) Successful standing-up motion; (right) standing robot with weight*

If the robot fell over after viewing the object, this was regarded as a failure. The robot could not move its upper body because it was fixed in place, so the robot was provided with a barbell-shaped weight, and the robot's arm followed the subject's arm. The subjects were instructed to move their arms for balance and to make the robot stand up successfully. The number of trials needed to achieve this and the trajectory of the head height during the standing up motion were recorded.

The time when the subject began moving the right hand was taken as the start of the standing exercise and, the time when the head height showed the maximum value was taken as the end.

4.3.2. Results and discussion for Experiment 1

Figure 8 shows the CoGs of the robot when it successfully stood up and the subject performing the original standing-up motion. The CoG of the robot was calculated by assuming that the foot of the robot was stable and the robot stood without tilting. The CoG of the robot was obtained by combining the data from the servomotors, balancer struts, and centroid position vector of the weight held in the hand. Given that other parts were lighter than the servomotors, they were not considered. The CoG of the person was at the midpoint between the head and feet. The heel of the robot was set at 0 mm, and the human was plotted at a scale of 1/4 for comparison. The view-point heights of the human and robot are shown in the lower part of Figure 9. We also scaled down the human to 1/4 based on the distances from the foot to the head. Figure 9 shows the

stretched abscissa from Figure 8 based on the original standing-up motion of the subject.

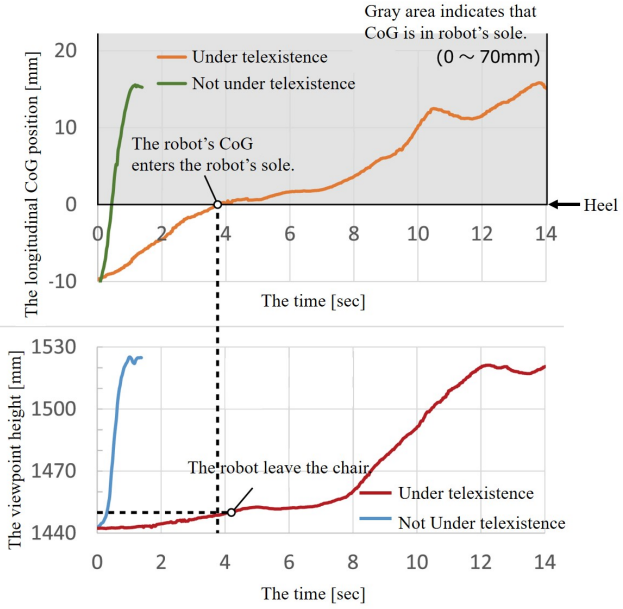

Figure 8: *CoG position and viewpoint height while standing up. With telexistence, the outside world is seen through the robot's cameras, so the position is apparently under 4 G. Without telexistence, the outside world is seen without the HMD, so the position is under 1 G.*

Given that the heel of the robot was set as 0 mm, the CoG was within the bottom of the shoe between 0 and 70 mm as long as the shoe did not tilt and was in contact with the ground. The waist of the robot moved away from the chair when the viewpoint height of the person was greater than 1450 mm. This is because the body posture of the robot remained unchanged.

Fourteen trials were need before the robot successfully stood up. The time taken was 12.1 s, and the maximum viewpoint height of the robot was 0.373 m. In the sitting position, the CoG of the robot was behind the heel. However, bringing the hand forward shifted the CoG to the bottom of the shoe at 3.74 s. Subsequently, the subject raised the waist at 4.15 s. This moved the CoG into the sole of the shoe, and the standing-up motion was performed with the CoG staying within the sole of the shoe. This standing-up motion was therefore performed while static stability was maintained.

With the original standing-up motion of the subject, the robot left the chair 0.30 s before the CoG entered the foot at 0.45 s. Given that the CoG did not move to the rear of the shoe when the waist was raised, the subject standing up used dynamic stability rather than static stability, in contrast to the previous subject.

These results show that, although the standing-up motion was performed under an apparent gravity of 4 G, the standing-up motion based on dynamic stability as normally performed by the subject could not be reproduced.

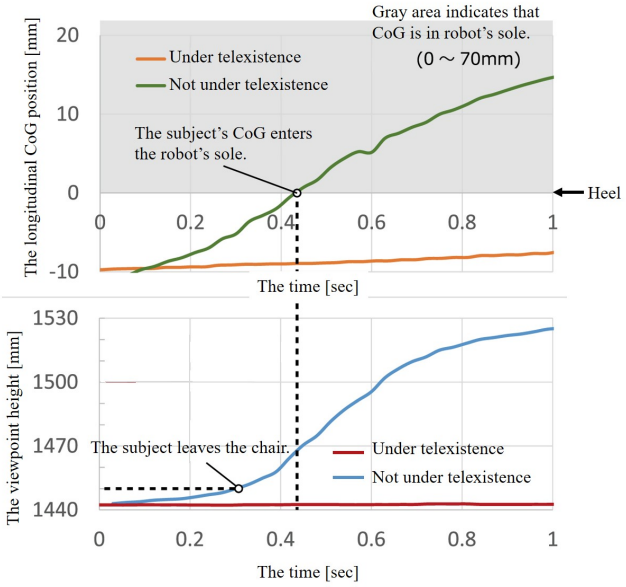

Figure 9: *CoG position and viewpoint height of the subject.*

We considered the standing up to be successful based on our hypothesis. By expanding Equation (7) to include the moment of inertia $\boldsymbol{I}_{HT}$ and angular acceleration $\dot{\boldsymbol{\omega}}_{HT}$ for the upper body motion of the human, the following is obtained:

$$\boldsymbol{I}_H\dot{\boldsymbol{\omega}}_H - \boldsymbol{I}_{HT}\dot{\boldsymbol{\omega}}_{HT} = -m\boldsymbol{T}_s + \boldsymbol{k} \tag{22}$$

For the robot, if the equation is similarly expanded with the moment of inertia $\boldsymbol{I}_{1T}$ and angular acceleration $\dot{\boldsymbol{\omega}}_{1T}$, the following is obtained:

$$\boldsymbol{I}_1\dot{\boldsymbol{\omega}}_H - \boldsymbol{I}_{1T}\dot{\boldsymbol{\omega}}_{1T} = -m\boldsymbol{T}_a + \boldsymbol{k}' \tag{23}$$

From these two equations, the following conditions can be satisfied by the movement of the upper body, similar to gravity compensation.

$$\dot{\boldsymbol{\omega}}_1 = \dot{\boldsymbol{\omega}}_H \tag{24}$$

Given that the upper body was fixed in this experiment, the subject appears to have successfully stood up by acquiring the skill of adjusting the CoG by shifting weight.

4.4. Experiment 2: Standing-up motion replay

In order to verify the effect of the control law, a person was asked to stand upright under a gravitational acceleration of 1 G, and the motions of the head and toe were recorded. According to the control law, we then made the 1/4-scale robot follow the posture of the recorded motion.

In this experiment, the locus of the viewpoint height was compared under three conditions: apparent gravity compensation (1 G), no apparent gravity compensation (4 G), and the recorded motion replayed ideally without leaning.

The height of the chair, the robot body, and the human's parameters were the same as those in Experiment 1. The balancer had a

mass of 0.475 kg at the tip of the 0.350 m link. The height of the head of the robot under both conditions was measured with recording markers placed on the top of the head using Opti Track.

4.4.1. Results and discussion for Experiment 2

Figure 10 shows the trajectory of the viewpoint height of the robot under each condition. Under the ideal follow-up condition, a maximum viewpoint height of 374 mm was recorded at 0.9 s. The viewpoint height at 0.9 s was 373 mm under an apparent gravity of 1 G and 363 mm under an apparent gravity of 4 G. Under an apparent gravity of 1 G, the trajectory followed a maximum delay of 17 ms with respect to the ideal orbit.

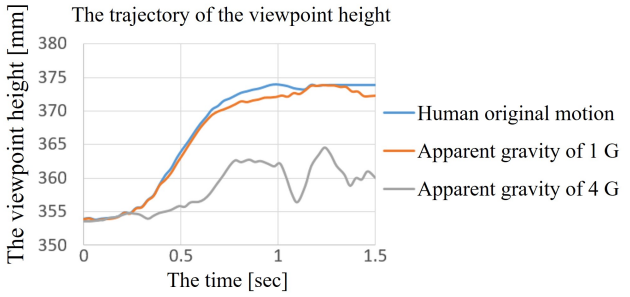

Figure 10: *Trajectory of the viewpoint height under each condition.*

Figure 11 shows the posture of the robot under the apparent gravities of 4 G and 1 G at 0.9 s. Figure 12 shows continuous frames of the robot standing up with apparent gravity compensation.

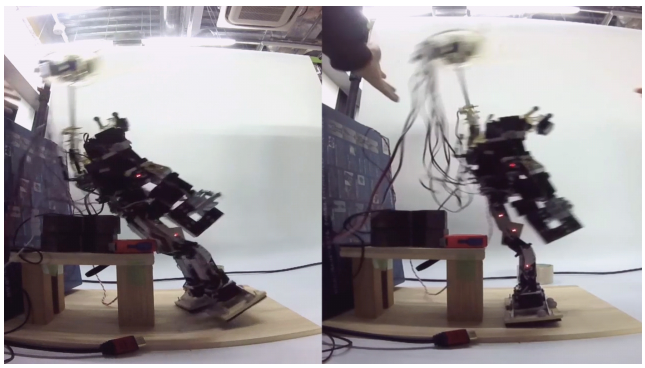

Figure 11: *Posture at 0.9 s: (left) without and (right) with gravity compensation.*

Under an apparent gravity of 4 G, the negative moment due to the CoG was large, so the sole of the foot floated. At 0.9 s, the waist and chair were in contact, but the robot failed to stand up. Under the apparent gravity of 1 G, there was no contact between the waist and chair at 0.9 s. Under the apparent gravity of 1 G, the standing-up motion was successfully performed because the viewpoint height was equivalent to the ideal condition at 0.9 s, and there was no ground point of the waist and chair at that time.

Figure 12 suggests that the balancer began moving from the

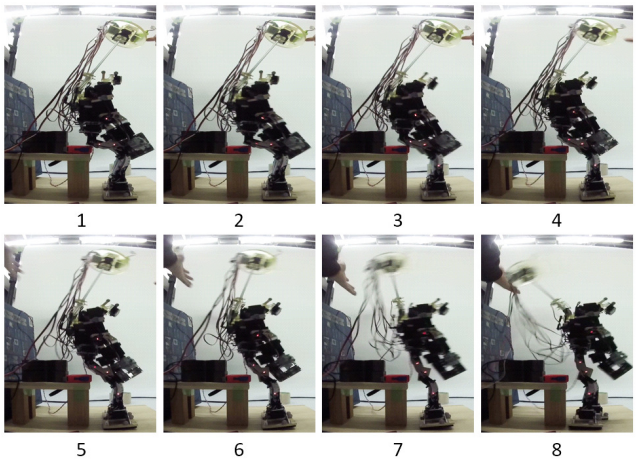

Figure 12: *Standing-up process of the robot with gravity compensation.*

fourth frame onwards (i.e., just before the waist left the chair), and the balancer began to move greatly after the waist rose from the chair. This indicates that the movement of the balancer was because of the gravity compensation, which contributed to the successful standing up.

Therefore, we successfully achieved the standing-up motion with apparent gravity compensation. However, we failed without apparent gravity compensation, which was expected from the difficulty of standing up under the apparent gravity of 4 G in Experiment 1.

With apparent gravity compensation, the robot's view-point reached the ideal height of 373 mm at 0.9 s without obtaining any visual feedback. In other words, this standing-up motion has an ideal standing-up time and equivalent viewpoint height. This is based on the standing-up ability demonstrated by the subject previously. Therefore, the standing-up motion can be transmitted by apparent gravity compensation.

Similar standing-up motions should be able to be generated even if visual feedback is given as long as people experience the visual flow through the robot. With apparent gravity compensation, humans should succeed in standing up when the viewpoint height and achievement time are equivalent to the human's original motion without practice. Therefore, compensating for the apparent gravity and performing the standing-up motion under a gravitational acceleration of 1 G is more effective than expecting human adaptation.

By considering the viewpoint height trajectory of the robot under an apparent gravity of 1 G, we achieved realism in the telexistence.

Between 0.0 and 0.7 s, the same viewpoint position was achieved with a maximum delay time of 17 ms. The maximum delay was 50 ms when the control period of 33 ms for this system is included. This is smaller than the delay of 80 ms that is allowed for a flight simulator with a visual display [WBW96]. For this standing-up motion, stability was felt with a delay of 50 ms or less [AHJ*01]. The presence was kept at least until 0.7 ms. Even between 0.7 s and 0.9 s, the polarity of the angular velocity did not change for the ideal

trajectory and under the apparent gravity of 1 G as a whole. Hence, the telexistence was preserved under an apparent gravity 1 G during this time.

The small robot used in this research reproduced the relative positions and posture of the human head and toe based on foot-eye coordination. Therefore, the robot's body does not reproduce the motion of humans who use the inertial force generated by moving the upper body to stand up. However, gravity compensation based on the equivalent physical constant hypothesis enabled the robot to stand up in a manner similar to that of a human. Hence, the equivalent physical constant condition can be applied not only to scale conversion but also as a means of absorbing the differences in DOF arrangement and mass distribution for a conventional life-size robot.

In this study, we performed a standing-up motion with a 1/4-scale robot. It should be possible to adapt the proposed hypothesis to make robots of other scales, such as larger than a human, perform the standing-up motion in the same way.

5. Limitation

The equivalent physical multiplier hypothesis scales the physical elements for scale conversion telexistence as described at the beginning of Section 3.1. In other words, this hypothesis converts changes in physical constants caused by differences in scales.

In principle, a mechanism capable of inputting and outputting the moment of three axes was designed. However, this study focused only on a simplified mechanism for sagittal plane movement in order to establish kinematic similarity.

6. Conclusion

We proposed an equivalent physical constant hypothesis and applied the equivalent gravity condition to 1/4-scale conversion telexistence. Given that the standing-up motion was confirmed, we obtained results supporting the equivalent physical constant hypothesis.

Acknowledgments

This research was in collaboration with the Komatsu MIRAI Construction Equipment Cooperative Research Center and supported by the Young Scientists (B) Grant Number 15H01699 and JST PRESTO Grant Number JPMJPR15D7.

References

[AHJ*01] ALLISON R. S., HARRIS L. R., JENKIN M., JASIOBEDZKA U., ZACHER J. E.: Tolerance of temporal delay in virtual environments. In *Proceedings IEEE Virtual Reality 2001* (March 2001), pp. 247–254. doi:10.1109/VR.2001.913793. 7

[BS11] BRUDER G., STEINICKE F.: Perceptual evaluation of interpupillary distances in head-mounted display environments. In *Proceedings of the GI-Workshop VR/AR* (2011), pp. 135–146. URL: http://basilic.informatik.uni-hamburg.de/Publications/2011/BS11a. 1, 2

[KI17] KIM J., INTERRANTE V.: Dwarf or Giant: The Influence of Interpupillary Distance and Eye Height on Size Perception in Virtual Environments. In *ICAT-EGVE 2017 - International Conference on Artificial Reality and Telexistence and Eurographics Symposium on Virtual Environments* (2017), Lindeman R. W., Bruder G., Iwai D., (Eds.), The Eurographics Association. doi:10.2312/egve.20171353. 1, 2

[Spa70] SPADY A. A.: Comments on several reduced-gravity simulators used for studying lunar self-locomotive tasks. In *NASA Technical Note* (1970). URL: https://ntrs.nasa.gov/archive/nasa/casi.ntrs.nasa.gov/19700016856.pdf. 1, 2

[Tac15] TACHI S.: *Telexistence*. Springer International Publishing, Cham, 2015, pp. 229–259. URL: https://doi.org/10.1007/978-3-319-17043-5_13, doi:10.1007/978-3-319-17043-5_13. 1

[TKS*03] TACHI S., KOMORIYA K., SAWADA K., NISHIYAMA T., ITOKO T., KOBAYASHI M., INOUE K.: Telexistence cockpit for humanoid robot control. *Advanced Robotics 17*, 3 (2003), 199–217. URL: https://doi.org/10.1163/156855303764018468, doi:10.1163/156855303764018468. 1

[ToLTK90] TAKANISHI A., OK LIM H., TSUDA M., KATO I.: Realization of dynamic biped walking stabilized by trunk motion on a sagittally uneven surface. In *EEE International Workshop on Intelligent Robots and Systems, Towards a New Frontier of Applications* (July 1990), pp. 323–330 vol.1. doi:10.1109/IROS.1990.262408. 1

[TTK*07] TSETSERUKOU D., TADAKUMA R., KAJIMOTO H., KAWAKAMI N., TACHI S.: Intelligent variable joint impedance control and development of a new whole-sensitive anthropomorphic robot arm. In *2007 International Symposium on Computational Intelligence in Robotics and Automation* (June 2007), pp. 338–343. doi:10.1109/CIRA.2007.382885. 1, 2

[TTKK90] TAKANISHI A., TAKEYA T., KARAKI H., KATO I.: A control method for dynamic biped walking under unknown external force. In *EEE International Workshop on Intelligent Robots and Systems, Towards a New Frontier of Applications* (July 1990), pp. 795–801 vol.2. doi:10.1109/IROS.1990.262498. 1

[WBW96] WILDZUNAS R., BARRON T., WILEY R.: Visual display delay effects on pilot performance. *Aviat Space Environ Med. 67*, 3 (1996), 214–221. 7

[YT02] YANAGIDA Y., TACHI S.: Dynamic effects of inconsistent field of view in hmd-based telexistence systems. *Transactions of the Virtual Reality Society of Japan 7*, 1 (2002), 69–78. doi:10.18974/tvrsj.7.1_69. 1, 2

[YTK93] YAMAGUCHI J. ., TAKANISHI A., KATO I.: Development of a biped walking robot compensating for three-axis moment by trunk motion. In *Proceedings of 1993 IEEE/RSJ International Conference on Intelligent Robots and Systems (IROS '93)* (July 1993), vol. 1, pp. 561–566 vol.1. doi:10.1109/IROS.1993.583168. 1